

This discussion paper is/has been under review for the journal *Climate of the Past* (CP).
Please refer to the corresponding final paper in CP if available.

South-western Africa vegetation responses to atmospheric and oceanic changes during the last climatic cycle

D. H. Urrego^{1,2}, M. F. Sánchez Goñi¹, A. L. Daniou³, S. Lechevrel⁴, and V. Hanquiez⁴

¹Ecole Pratique des Hautes Etudes EPHE, Université de Bordeaux, Environnements et Paléoenvironnements Océaniques et Continentaux (EPOC), Unité Mixte de Recherche 5805, 33615 Pessac, France

²Geography, College of Life and Environmental Sciences, University of Exeter, UK

³Centre National de la Recherche Scientifique CNRS, Université de Bordeaux, Environnements et Paléoenvironnements Océaniques et Continentaux (EPOC), Unité Mixte de Recherche 5805, 33615 Pessac, France

⁴Université de Bordeaux, Environnements et Paléoenvironnements Océaniques et Continentaux (EPOC), Unité Mixte de Recherche 5805, 33615 Pessac, France

Received: 14 December 2014 – Accepted: 26 January 2015 – Published: 16 February 2015

Correspondence to: D. H. Urrego (d.urrego@exeter.ac.uk)

Published by Copernicus Publications on behalf of the European Geosciences Union.

345

Abstract

Terrestrial and marine climatic tracers from marine core MD96-2098 collected in the southwestern African margin and spanning from 194 to 24 (thousand years before present) documented three pronounced expansions of Nama-Karoo and fine-leaved savanna during the last interglacial (Marine Isotopic Stage 5 – MIS 5). Nama-Karoo and fine-leaved savanna expansions were linked to increased aridity during the three warmest substadials of MIS 5. Enhanced aridity potentially resulted from a combination of reduced Benguela Upwelling System (BUS), expanded subtropical high-pressure cells, and reduced austral-summer precipitation due to a northward shift of the Intertropical Convergence Zone (ITCZ). Decreased austral-winter precipitation was likely linked to a southern displacement of the westerlies. In contrast, during glacial isotopic stages MIS 6, 4 and 3, Fynbos expanded at the expense of Nama-Karoo and fine-leaved savanna indicating a relative increase in precipitation probably concentrated during the austral winter months. Our record also suggested that warm-cold or cold-warm transitions between isotopic stages and substages were punctuated by short increases in humidity. Increased aridity during MIS 5e, 5c and 5a warm substages coincided with minima in both precessional index and global ice volume. On the other hand, austral-winter precipitation increases were associated with precession maxima at the time of well-developed northern-hemisphere ice caps.

1 Introduction

Southern Africa is influenced at present by tropical and subtropical atmospheric circulation linked to ITCZ shifts, and by both the Indian and the Atlantic Oceans (Tyson and Preston-Whyte, 2000). The water exchange between the two oceans is termed the Agulhas leakage and is suggested as a potential trigger of meridional overturning circulation changes (Beal et al., 2011; Biastoch et al., 2008). BUS also affects climate in southwestern Africa and its strength is linked to arid conditions and to the extent of the

346

coastal Namib Desert (Cowling et al., 1997b). The combination of globally-important atmospheric and oceanic systems linked to the climate of southern Africa make understanding past climate change in the region particularly significant.

5 Whether southern Africa was characterised by aridity or by increased humidity during the last interglacial remains unclear. Previous work using marine markers has documented an intensification of the Agulhas leakage during interglacials (Peeters et al., 2004), which suggests a reduced influence of the subtropical front and reduced precipitation. Other works have shown increased sea surface temperatures (SST) in the Benguela Current during interglacials linked to weakening of BUS (Kirst et al., 1999) and decreased influence of the ITCZ in southern Africa (Tyson, 1999) suggesting its northward migration. These three climatic factors combined would result in a slight increase in humidity in northeastern South Africa during interglacials. On the other hand, increased aridity during the last interglacial in southern Africa has been suggested based on ratios of aeolian dust and fluvial mud in marine sediments (Stuut and Lamy, 15 2004).

Vegetation-based climate reconstructions for southern Africa have been less straight forward given the paucity of records (Dupont, 2011) and fragmentary nature of some terrestrial sequences (Scott et al., 2012; Meadows et al., 2010). On one hand, some records point to expansions of the Fynbos biome (Shi et al., 2001) and the winter-rainfall zone during glacial periods (Chase and Meadows, 2007), and to a contracting Namibian Desert during interglacials (Shi et al., 2000) and the late Holocene (Scott et al., 2012). On the other hand, it has been suggested that savannas expanded southwards during the Holocene climate optimum (Dupont, 2011), and that the southern Africa summer-rainfall zone expanded during interglacials due to a strengthening of the walker circulation and a southward migration of the ITCZ (Tyson, 1999). Contrastingly, significant reductions of austral-summer precipitation in southern Africa are suggested to coincide with precession minima both during glacials and interglacials (Partridge et al., 1997), and are independently supported by reductions of grass-fuelled fires in the subcontinent (Daniau et al., 2013). The latter observations suggest aridity increase 20 25

347

and savanna biome reductions, instead of expansions, during the last interglacial precession minima. Whether the last interglacial was characterised by orbitally-driven increased aridity or increased precipitation may have significant implications for resource availability and climate in the region today, hence the importance of further investigating the glacial–interglacial climate and vegetation dynamics of southern Africa. 5

In this study we aim to disentangle the contrasting hypotheses of orbital-scale climate change in southern Africa by combining terrestrial and marine tracers from the marine sequence MD96-2098. We use pollen and charcoal as terrestrial tracers, and $\delta^{18}\text{O}$ from benthic foraminifera as a marine tracer. Vegetation reconstructions from marine records have contributed to our understanding of ocean-land interactions in many regions of the world, including the Iberian Peninsula (Sánchez Goñi et al., 2000), the eastern subtropical Pacific (Lyle et al., 2012), and the tropical Atlantic (González and Dupont, 2009). Studies from the African margin (e.g. Dupont, 2011; Dupont and Behling, 2006; Hooghiemstra et al., 1992; Leroy and Dupont, 1994) have demonstrated that pollen records from marine sequences are reliable and useful tools to reconstruct changes in the regional vegetation of adjacent landmasses and the climate dynamics at orbital and suborbital timescales. In arid environments, marine sequences are particularly essential in providing continuous records of vegetation change at the regional scale. 10 15

The pollen sequence from MD96-2098 presented here covers the period between 24 and 190 ka and provides an integrated picture of past regional vegetation changes in southwestern Africa. Southwestern Africa refers here to the western half of South Africa and Namibia that is drained by the Orange River. We compare vegetation-based atmospheric changes with independent climatic markers from the same marine sequence, along with other regional records for oceanic conditions and global ice dynamics, to reconstruct atmospheric and oceanic configurations around southern Africa for MIS 6, 5, 4 and 3. 20 25

348

2 Modern environmental setting

The southwestern part of the African continent (Atlantic side) is influenced by the seasonal migration of the subtropical front and the southern westerlies that bring precipitation during the austral-winter months (Beal et al., 2011). Precipitation in southwestern Africa is additionally controlled by the cold Benguela current and wind-driven upwelling that results in aridity on the adjacent continent (Stuut and Lamy, 2004). In the Indian Ocean, warm waters from the Agulhas current (Beal and Bryden, 1999) and austral-summer heat enhance evaporation and result in relatively high precipitation in southeastern Africa and the interior of the continent (Fig. 1). Austral-summer precipitation is also linked to the position of tropical low pressure systems (e.g. ITCZ) and reduced subtropical high pressure (Tyson and Preston-Whyte, 2000). As tropical low-pressure systems migrate northwards during the austral winter, subtropical high pressure significantly reduces austral-summer precipitation in southern Africa. This climatic configuration broadly determines the vegetation distribution in southern Africa. Phyto-geographical regions were initially classified by White (1983), and later revisited and described into seven biome units by Rutherford (1997). These include the Succulent-Karoo, Nama-Karoo, Desert, savanna, Fynbos, Grassland, and forest (Fig. 1).

The Succulent-Karoo receives between 20 and 290 mm yr⁻¹ of which more than 40 % falls during the austral-winter months (Rutherford, 1997). The two most abundant succulent families are Crassulaceae and Mesembryanthemaceae, and non-succulents are Anacardiaceae, Asteraceae, and Fabaceae (Milton et al., 1997). C4 perennial grasses (Poaceae) have relatively low abundance in the Succulent-Karoo (Milton et al., 1997).

The Nama-Karoo receives precipitation from 60 to 400 mm yr⁻¹ falling primarily during the austral summer (Palmer and Hoffman, 1997). Vegetation is characterized as dwarf open shrub land with high abundance of Poaceae, Asteraceae, Aizoaceae, Mesembryanthemaceae, Liliaceae and Scrophulariaceae (Palmer and Hoffman, 1997). Grasses from the Poaceae family can be particularly dominant in the Nama-Karoo biome (Fig. 2a). The Nama- and Succulent-Karoo are structurally similar but influenced

349

by different seasonal precipitation (Rutherford, 1997). The Nama-Karoo is influenced primarily by austral summer precipitation, while the distribution of the Succulent-Karoo coincides with the austral-winter rainfall region (Chase and Meadows, 2007). To the northwest, the Nama-Karoo biome transitions into the Desert, where mean annual precipitation can be as low as 20 mm yr⁻¹ (Jurgens et al., 1997). The Desert reaches 300 km inland and its extent is linked to the intensity of BUS (Lutjeharms and Meeuwis, 1987).

High precipitation seasonality (i.e. difference between dry-season and rainy-season precipitation) and high austral-summer rainfall characterize the savanna. The savanna biome represents a mosaic that includes shrublands, dry forests, lightly-wooded grasslands, and deciduous woodlands (Scholes, 1997). At the landscape scale however, the savanna can be subdivided into the fine- and broad-leaved savannas based on moisture conditions and soils (Scholes, 1997). The fine-leaved savanna (Fn-LSav) is found in dry and fertile environments (between 400 and 800 mm yr⁻¹), and the broad-leaved savanna (Bd-LSav) is found in nutrient-poor and moist environments (up to 1500 mm yr⁻¹) (Scholes, 1997). Additionally, in the Fn-LSav fuel load and fire frequency are very low, while Bd-LSav has high fuel load and fire frequency (Scholes, 1997; Archibald et al., 2010). The Fn-LSav is found to the northeast of the Nama-Karoo biome (Fig. 1), known as the Kalahari Highveld transition zone (Cowling and Hilton-Taylor, 2009). Due to the transitional character of the Fn-LSav, some of its outer parts have been classified as grassland or Nama-Karoo (White, 1983). The composition of the Fn-LSav can be similar to that of the Nama-Karoo, with dominance of C4 grasses (Poaceae) and succulent plants, but it differs in having scattered trees (Fig. 2b) (Cowling et al., 1994). The Bd-LSav is characterized by broad-leaved trees from the Caesalpiniaceae and Combretaceae families and an understory dominated by grasses (Scholes, 1997).

The grassland biome is dominated by C4 grasses and non-grassy forbs as *Anthospermum* sp., *Lycium* sp., *Solanum* sp. and *Pentzia* sp. (O'Connor and Bredenkamp, 1997). At the high elevations the biome is dominated by C3 grasses. In the grass-

350

lands, precipitation is highly seasonal with mean annual rainfall ranging between 750 and over 1200 mm, falling primarily during the austral-summer months (O'Connor and Bredenkamp, 1997) (Fig. 1).

The southernmost part of Africa is characterised by the Fynbos biome, a fire-prone vegetation dominated by Ericaceous and Asteraceae shrubs, diverse *Protea* shrubs and trees, and Restionaceae herbs (Cowling et al., 1997a). The Fynbos biome receives relatively high annual precipitation (1200 mm year⁻¹) concentrated during the austral-winter months (Rutherford, 1997). The coastal forest biome is found along the eastern coast of the subcontinent and often occurs in small patches with high abundance of *Podocarpus* (Rutherford, 1997). *Podocarpus* patches can also be found in the southeastern part of the Fynbos.

3 Materials and methods

3.1 Marine core description and pollen analysis

Pollen analysis was conducted on marine core MD96-2098 (25°36' S, 12°38' E). This giant CALYPSO core was collected during the IMAGES II-NAUSICAA cruise at a 2910 m water depth from the Lüderitz slope in the Walvis Basin, approximately 500 km northwest of the Orange River mouth (Fig. 1). The sediments of this 32 m long core were composed of calcium carbonates (foraminifera), biogenic silica (nannofossil mud), clays and organic matter (Bertrand et al., 1996). The core was sampled every 10 cm between 450 and 1940 cm (uncorrected depth) for pollen analysis. The uncorrected depth did not take into account artificial gaps created during piston extraction (Bertrand et al., 1996).

Sample volumes were estimated by water displacement. Pollen concentrations per unit volume were calculated based on a known spike of exotic *Lycopodium* spores added to each sample. Pollen extraction techniques included treatment with hydrofluoric and hydrochloric acids, and sieving through 150 and 10 µm filters. This filtration

351

allowed eliminating small non-palynomorph particles and concentrating pollen grains and spores. An independent test of this protocol showed that the use of a 10 µm sieve had no effect on the pollen composition of marine samples, i.e. comparison of filtered and unfiltered sample counts showed that taxa were not selectively filtered out during pollen preparation and concentration (see <http://www.ephe-paleoclimat.com/ephe/Lab%20Facilities.htm> for a detailed pollen preparation protocol).

We used the pollen spectra from 31 surface samples collected along a transect (Fig. 1) from Cape Town (South Africa) to Lüderitz (Namibia) and designed to cover the four major biomes of southwestern Africa (Table S1). The transect included samples from the Desert, Fynbos, Nama- and Succulent-Karoo. The samples were treated with standard acetolysis (Faegri and Iversen, 1989) and scanned under the microscope until completing pollen sums were greater than 300 grains (Supplement). We also used previously-published pollen spectra from 150 additional surface samples collected between 22° and 35° latitude south (APD, Gajewski et al., 2002). These pollen spectra were used to assess the distribution of Poaceae pollen percentages and other potential indicators of large biomes in southern Africa. ArcGIS 10 was used to draw iso-lines of pollen percentages by interpolating values from a total of 178 surface samples through the natural neighbour method. Additionally, we analysed two marine pollen samples from the upper part of core MD96-2098 (at 5 and 10 cm depth). We compared the pollen spectra from these core top samples with the pollen signal of the modern vegetation to evaluate how well marine sediments represent the vegetation of the adjacent landmasses, and to aid interpretation of the pollen record.

Pollen identification was aided by the pollen reference collection of the Department of Plant Sciences at University of the Free State (Bloemfontein, South Africa), the African Pollen Database (APD) (<http://medias3.mediasfrance.org/pollen>), the Universal Pollen Collection (<http://www.palyno.org/Pollen>), and pollen descriptions published by Scott (1982). Pollen grains from the Asteraceae family were grouped into three pollen taxa: *Artemisia*-type, *Stoebe*-type and other morphotypes were classified into Asteraceae-other. Some morphotypes were grouped into family types: Acanthaceae,

352

Chenopodiaceae-Amaranthaceae, Crassulaceae, Cyperaceae, Ericaceae, Myrtaceae, Ranunculaceae, Restionaceae, and Solanaceae.

To summarize changes in the fossil pollen record, detrended correspondence analysis (DCA) was used in tandem with non-metric multidimensional scaling (NMDS) as parametric and non-parametric alternatives (McCune and Grace, 2002). Results from the DCA ordination were preferred when NMDS was unable to reach a stable solution after several random starts, and when stress levels were too high to allow a meaningful interpretation (McCune and Grace, 2002). These ordinations were performed filtering out pollen morphotypes that only occurred in one sample to avoid overweighting rare taxa.

3.2 Marine core chronology

Two sediment gaps between 693 and 709 cm and 759 and 908 cm were described in the core log. These gaps were considered artificial and linked to piston extraction (Bertrand et al., 1996), thus the record could be assumed continuous. Depths were corrected to take into account these artificial sediment gaps. An age model was established for the record based on 16 marine isotope events (MIE) from the *Cibicides wuellerstorfi* $\delta^{18}\text{O}$ benthic record of MD96-2098 (Bertrand et al., 2002) and 14 Accelerator Mass Spectrometer radiocarbon ages (AMS ^{14}C) from mixed planktonic foraminifera extracted from MD96-2098 (Table S1). The 14 AMS ^{14}C dates were produced at the Laboratoire de Mesure du Carbone 14. One single ^{14}C date showed an age reversal and was therefore excluded from the chronology on the principle of parsimony. AMS ^{14}C ages were calibrated using the marine09.14c curve (Hughen et al., 2004) from CALIB REV5.0 (Reimer et al., 2013). We applied a 400 year global reservoir correction factor and a weighted mean Delta R of 157 years derived from 9 regional reservoir error values from the Marine Reservoir Correction Dataset (Dewar et al., 2012; Southon et al., 2002). MIE ages were derived from LR04 global stack (Lisiecki and Raymo, 2005) and additional sources (Henderson and Slowey, 2000; Drysdale et al., 2007; Waelbroeck et al., 2008; Masson-Delmotte et al., 2010; Sanchez Goñi and

353

Harrison, 2010) (Fig. S1). Sample ages were calculated using a linear interpolation between AMS ^{14}C ages and MIE using the R package PaleoMAS (Correa-Metrio et al., 2010).

4 Results and discussion

4.1 Pollen preservation and sources in marine core MD96-2098

Pollen sums excluding spores range from 100 to 240 grains in 141 samples analysed from core MD96-2098. The mean number of taxa per sample was 21. Total pollen concentration ranged between ca. 300 and 16 000 grains cm^{-3} during most of MIS 6, 5 and 3 and increased up to 48 000 grains cm^{-3} during MIS 4 (Fig. S2). The MIS5 pollen concentrations were comparable to those found in other oceanic margins (Sánchez Goñi et al., 1999), even though BUS facilitates preservation of pollen grains and other organic microfossils at this site (Bertrand et al., 2003). The low net primary productivity that characterizes southwestern Africa (Imhoff et al., 2004) could explain relatively low pollen concentrations in the continental margin (Fig. S2).

Pollen grains are part of the fine sediment fraction and can be transported by two main vectors: aeolian or fluvial (Hooghiemstra et al., 1986; Heusser and Balsam, 1977). Dupont and Wyputta (2003) modelled present-day wind trajectories for marine core locations between 6 and 30° S along the coastline of southern Africa. They suggest aeolian pollen input to the Walvis area (23° S) via the south-east trade winds during austral summer, and dominant east-to-west wind directions during the austral fall and winter. These winds transport pollen and other terrestrial particles from the Namib Desert, southern Namibia and western South Africa. The direction of the winds indicate that the Namib Desert, Nama-Karoo and Succulent-Karoo are the most likely sources of pollen in the Walvis area (Dupont and Wyputta, 2003). The authors also infer that south of 25° S wind directions are predominantly west to east and aeolian terrestrial input very low. Marine site MD96-2098 is located less than a degree south of the area

354

determined by Dupont and Wyputta (2003) to be dominated by terrestrial aeolian input. However, given that this threshold was established using only two marine sites located 6° apart at 23°26' (GeoB1710-3) and 29°27' (GeoB1722-1), it is difficult to conclude that MD96-2098 only receives wind-transported pollen.

MD96-2098 likely receives fine sediments from the Orange River plume. Sedimentological analyses of the Orange River delta and plume indicate that fine muds are transported both northwards and southwards (Rogers and Rau, 2006). Additionally, an analysis of the imprint of terrigenous input in Atlantic surface sediments found relatively high Fe/K values along the Namibian and South African margin that could reflect the input of Orange River material (Govin et al., 2012). Pollen grains are hence likely to reach the coring site from the Orange River catchment area.

Scott et al. (2004) argue that pollen in marine sediments can be the result of long-distance transport by ocean currents, suggesting that pollen assemblages in marine sediments do not reflect accurately past changes in vegetation and climate. However, the highest pollen influx in marine sediments along this margin is near the coast and the vegetation source (Dupont et al., 2007), not along the paths of oceanic currents (i.e. Benguela Current). Additionally, analyses of pollen transport vs. source in northwestern Africa show that pollen grains can sink rapidly in the water column (Hooghiemstra et al., 1986) before they can be carried away by ocean currents. As a result, influence of oceanic currents on the composition of pollen assemblages is probably negligible. Overall, the marine site MD96-2098 might receive both aeolian and fluvial pollen input from the vegetation located east and southeast to the site.

The pollen composition of the two core-top samples from core MD96-2098 are dominated by Poaceae (30 and 40%), Cyperaceae (20%) and Chenopodiaceae-Amaranthaceae (20 and 30%) (Fig. S2). This composition corresponds well with the pollen spectra from the three major biomes occupying today the adjacent landmasses (Fig. 1a): Desert, Nama-Karoo and Fn-LSav (Figs. S3 and 5). Pollen percentages from Fynbos taxa are less than 10%, *Podocarpus* is weakly represented, and taxa specifically found in the broad-leaved savanna (e.g. Caesalpinaceae, Combretaceae) are not

355

recorded. These results support the assumption that the main pollen source for marine core MD96-2098 is the vegetation from southwestern Africa.

4.2 Distribution and interpretation of Poaceae pollen in terrestrial and marine surface samples

Occurrence of Poaceae pollen in all surface samples corresponds to the presence of grass species in virtually all southern African biomes (Cowling et al., 1997b). Altogether, the spatial distribution of Poaceae pollen percentages appears to be essential information to distinguish the pollen signal from major biomes, and therefore climatic zones, in this region. In the eastern and northeastern part of southern Africa, the highest percentages of Poaceae pollen (up to 90%) are found in the pollen rain of the Bd-LSav and grasslands. In the western half of southern Africa, Poaceae pollen percentages in terrestrial surface samples are up to 60% in the Nama-Karoo and its transition with the Fn-LSav (Fig. 3). This suggests an overrepresentation of Poaceae in the pollen rain of the Nama-Karoo biome where grasses can be abundant but are not necessarily dominant.

Poaceae is likely to be well represented in other parts of the Fn-LSav, but the paucity of surface samples from this biome hinder drawing further conclusions. In the Namib Desert where abundance of grasses in the vegetation is low, Poaceae pollen percentages are as high as 25% in surface samples, comparable to 20% reported from hyrax dung (Scott et al., 2004).

In marine surface samples along the southwestern African coast, Poaceae pollen percentages are as low as 10% in samples collected in front of the Bd-LSav at around 15° S (Fig. 3). Poaceae pollen percentages increase to the South and the highest values (40%) are found between 20 and 25° S (Dupont and Wyputta, 2003) and correspond well with the distribution of the Desert and the Fn-LSav on the continent. The Poaceae pollen percentages from the two core-top samples from MD96-2098 may be used to extend the iso-lines drawn by Dupont and Wyputta (2003) to 25.5° S, showing that Poaceae pollen percentages are between 30 and 40% in front of the Desert,

356

Nama-Karoo and Fn-LSav biomes. As Poaceae pollen percentages in Desert surface samples are less than 25 %, high percentages of grass pollen from marine sediments in the southwestern Africa margin should be interpreted as indicator of the Nama-Karoo and the Fn-LSav, where Poaceae is as high as 70 % in terrestrial surface samples. Our field observations also support this view as we observed large grass-dominated vegetation in the Nama-Karoo and Fn-LSav. (Fig. 2).

4.3 Southwestern Africa vegetation and climatic changes from MIS 6 to 2

The pollen record presented here spans from 24.7 to 190 ka. A log transformation of concentration values in MD96-2098 results in a curve remarkably similar to that of $\delta^{18}\text{O}_{\text{benthic}}$ values (Fig. 4) and may be linked to changes in pollen input at the coring site. Relative increases in pollen concentration could indicate an increase in pollen arrival during low sea-level stands when the vegetation source was closest (i.e. during glacial stages). However, this is unlikely because of the width of the Walvis continental Shelf (i.e. rapid depth change in a few kilometres). An increase of pollen concentration might indicate instead an increase in pollen input during glacials, and/or an increase in pollen preservation linked to upwelling enhancement as suggested by Pichevin et al. (2005). Glacial–interglacial pollen concentration variations have no effect on the interpretation of the pollen record which is based on relative frequencies, but they do indicate the influence of the obliquity signal in the pollen record from MD96-2098.

The axis scores on DCA1 reveal changes in the composition of pollen assemblages that also resemble variations in the $\delta^{18}\text{O}_{\text{benthic}}$ record (Fig. 4). DCA1 axis scores from MIS 5 and 3 are overall positive in value, while scores from MIS 6 and 4 are negative. A series of large-magnitude changes in DCA1 axis scores (i.e. when adjacent sample scores switch from positive to negative values) are also visible and increase in amplitude after ca. 100 ka. Such changes in DCA Axis1 scores are also observed during MIS 6 but are of lesser magnitude. Changes in DCA axis scores suggest significant changes in vegetation composition from one time step to the next.

357

Nama-Karoo and Fn-LSav pollen percentages are up to 60 % during MIS 5 and display three percentage peaks that correspond with $\delta^{18}\text{O}_{\text{benthic}}$ and precession minima (Fig. 4a). These percentage peaks are centred at 125, 107 and 83 ka. The composition of pollen spectra from warm marine substages MIS 5e, 5c and 5a is comparable to the core-top samples (Fig. S2) and corresponds well with the modern pollen spectra from Nama-Karoo and Fn-LSav (Fig. S3). At the same time, Nama-Karoo and Fn-LSav pollen percentages in the core-top samples are relatively low compared to their maximum during MIS 5e (Fig. 4b).

During MIS 6 and 4, Nama-Karoo and Fn-LSav percentages are reduced and covary with $\delta^{18}\text{O}_{\text{benthic}}$ values. Pollen percentages of Chenopodiaceae-Amaranthaceae and Asteraceae-other are relatively high and increase along with enriched $\delta^{18}\text{O}_{\text{benthic}}$ values during MIS 6 and at the end of MIS 4 (Fig. S2). Cyperaceae pollen percentages vary throughout the record and are as high as 40 % during MIS 4. Fynbos indicators (Ericaceae, *Passerina*, *Anthospermum*, *Cliffortia*, and *Protea Artemisa*-type and *Stoebe*-type) show relative increases in pollen percentage during MIS 6, 4 and 3 (Figs. 4b and S2). Pollen percentages of Restionaceae increase after the 105 ka $\delta^{18}\text{O}_{\text{benthic}}$ minimum and remain abundant during the rest of MIS 5 through MIS 3, despite a relative decrease during MIS 4. *Podocarpus* percentages are lower than 10 % but show increases at stage boundaries around 135 ka (MIS 6/5), 100 ka (5c/5b), 75 ka (MIS 5a/4), 60 ka (MIS 4/3), and around 27 ka (MIS 3/2) (Fig. S2).

The increases of Nama-Karoo and Fn-LSav during MIS 5e, 5c and 5a suggest an increase in aridity in southwestern Africa that likely resulted from expansions in three directions (Fig. 5). The Nama-Karoo and Fn-LSav probably expanded to the northwest into the present-day area of the coastal Namib Desert as the intensity of BUS weakened during MIS 5 warm substages. This weakening has been documented through alkenone-based SST from marine core GeoB1711-3 (Kirst et al., 1999) (Fig. 4c), foraminifera-assemblage based SST (Chen et al., 2002) and grain-size end-member modelling (Stuut et al., 2002). Stuut and Lamy (2004) also suggested reduced atmospheric circulation and weakening of trade winds during interglacials compared to

358

glacials, resulting in a reduction of the wind-driven upwelling. A weakened BUS and the associated relative increase in humidity likely led to a colonization of Desert areas by Nama-Karoo or Fn-LSav (Fig. 5a). Comparable contractions of the Namib Desert linked to increased SSTs and weakening of BUS during the present interglacial are documented by Shi et al. (2000).

To the south, the Nama-Karoo and Fn-LSav likely expanded at the expense of the Succulent-Karoo and Fynbos. Warm Antarctica temperatures recorded during warm substages of MIS 5 (EPICA, 2006) would drive the southern westerlies polewards (Ruddiman, 2006), contributing to the ventilation of deep CO₂-rich waters in the southern Ocean (Toggweiler and Russell, 2008). This mechanism would explain the parallel-
ing trends observed between MIS 5 Nama-Karoo and Fn-LSav expansions in southern Africa and the atmospheric CO₂ record (Petit et al., 1999; Bereiter et al., 2012) (Fig. 5). A poleward migration of the westerlies during the present interglacial, relative to their position during the previous glacial, has been suggested by Weldeab et al. (2013), and correlated with nssCa²⁺ from Antarctica (Röthlisberger et al., 2008). Such poleward migration of the westerlies during the present interglacial is equivalent to the westerlies migration we propose for warmest periods of the last interglacial. The increased Agulhas leakage documented in the Cape basin record during the last interglacial (Peeters et al., 2004) (Fig. 4c) has been linked to a southward migration of the subtropical front and the westerlies, reducing austral-winter precipitation over southern Africa. Such an atmospheric configuration would in turn favour the development of the Nama-Karoo at the expense of Succulent-Karoo and Fynbos biomes (Fig. 5a).

To the northeast, Nama-Karoo and Fn-LSav likely pushed the limit of Bd-LSav equatorward as austral-summer precipitation decreased (Fig. 5a). Austral-summer precipitation reductions in Southern Africa have been linked to reduced austral-summer insolation in the Pretoria saltpan (Partridge et al., 1997) and to reductions of grass-fuelled fires during precession minima reconstructed from MD96-2098 (Daniau et al., 2013) (Fig. 4b). Increased northern-hemisphere insolation during MIS 5 warm substages would drive the ITCZ northwards while subtropical high pressure cells over the

south Atlantic and the Indian Oceans would expand (Fig. 5a) (Ruddiman, 2006). Such changes in the tropical and subtropical pressure systems would allow the expansion of the Nama-Karoo and Fn-LSav to the northeast.

In contrast with the results presented here, previous studies report poleward interglacial expansions of savannas based on pollen records from marine sediments along the southwestern African coast (Dupont, 2011). However, these studies univocally interpret the Poaceae pollen percentage increases as the result of savanna expansions. Such an interpretation is potentially plausible in marine records collecting pollen from broad-leaved savanna vegetation, e.g. the Limpopo basin (Dupont et al., 2011). However, our study shows that Poaceae pollen percentage increases in sequences located off the southwestern African coast can alternatively indicate the expansion of fine-leaved savanna and Nama-Karoo vegetation. Previous studies do not differentiate between the broad-leaved and fine-leaved savannas, despite the significant climatic and structural differences between these two types of vegetation. The Bd-LSav is influenced by fire and receives a considerable amount of precipitation during the austral summer (Scholes, 1997). The Fn-LSav is structurally and climatically more similar to the Nama-Karoo biome, as it receives very low austral-summer precipitation and does not burn (Archibald et al., 2010) despite being under a regime of significant precipitation seasonality (Scholes, 1997). If high Poaceae pollen percentages during MIS 5 warm substages in our record were related with expansions of the Bd-LSav and increased summer precipitation, the fire activity should also increase during these substages. Instead, an independent charcoal record from the same marine sequence MD96-2098 (Fig. 4b) documents reductions of grass-fuelled fires and a decrease in austral-summer precipitation during MIS 5 precession minima (Daniau et al., 2013). An atmospheric configuration with reduced austral summer precipitation in Southern Africa and the ITCZ shifted northward during the warmest periods of MIS 5 is also consistent with documented strengthening of Asian monsoon and weakening of the South American monsoon during the last-interglacial precession minima (Wang et al., 2004).

Our results suggest that the Bd-LSav retreated equatorwards during MIS 5 precession minima, while Nama-Karoo and Fn-LSav expanded. Nama-Karoo and Fn-LSav probably covered a surface area larger than at present during MIS 5 warm substages, as indicated by up to 70% pollen from this biome during MIS 5 compared to 35% in the core-top samples. This is despite the difference in precession parameters between the last millennium and MIS 5 warm substages. Recent model experiments on the impact of precession changes on South African vegetation indicate that high precession is linked to reductions of the broad-leaved savannas (Wolfe et al., 2014). Altogether these vegetation changes point to increased aridity in southwestern Africa during the warmest periods of the last interglacial.

During glacial isotopic stages, contractions of the Nama-Karoo and Fn-LSav would result from a different atmospheric configuration (Fig. 5b): a southward migration of the ITCZ and the associated South African monsoon (Daniau et al., 2013; Partridge et al., 1997) increasing austral-summer rainfall over southern Africa; an intensification of BUS and decreased SST off the Namibian coast (Stuut and Lamy, 2004; Kirst et al., 1999) leading to aridification of coastal areas; and lastly, an equatorward migration of the westerlies increasing austral-winter precipitation and allowing a northward expansion of the winter-rain zone in Southern Africa (Chase and Meadows, 2007). The proposed glacial precipitation changes are consistent with recent estimates of Last Glacial Maximum palaeoprecipitation based on glacier reconstruction and mass-balance modelling (Mills et al., 2012), with leaf-wax reconstructions of hydroclimate (Collins et al., 2014), and with simulated glacial climatic fluctuations in southern Africa (Huntley et al., 2014).

The pollen record from MD96-2098 also suggested glacial expansions of Fynbos (Fig. 4b), as pollen percentages of *Artemisia*-type, *Stoebe*-type, *Passerina* and *Ericaceae* were higher during MIS 6, 4 and 3 than in the core-top samples (Fig. S2). These results were consistent with glacial northward expansions of Fynbos documented in other pollen records from southern Africa (Shi et al., 2000; Dupont et al., 2007). Our record also documented a large peak in Fynbos indicators (Fig. 4b) that coincided with a fast decrease in Nama-Karoo and fine-leaved savanna pollen percentages at the

361

MIS 5e/5d transition (c. 117 ka), a precession and eccentricity maxima (Laskar, 1990), and an accelerated cooling in Antarctica (EPICA, 2006; Masson-Delmotte et al., 2010) (Fig. 4c). As pollen percentages of *Artemisia*-type obtained from surface samples were associated with the Fynbos biome and austral-winter precipitation (Figs. S4 and 5), it cannot be discarded that these increases resulted from a rapid and short-lived expansion of the winter-rain zone of southern Africa. Transitions MIS 6/5 and 4/3 were characterized by small but rapid increases in *Podocarpus*, potentially linked to a short increase in annual precipitation. Such increases in *Podocarpus* have also been documented in other records from southern Africa (Dupont et al., 2011; Dupont, 2011).

Finally, the amplitude of millennial-scale vegetation changes increased between ca. 100 and 25 ka, and was highlighted by switches from negative to positive DCA1 scores (Fig. 4b) and increased variability of Restionaceae pollen percentages. These results could indicate either enhanced trade-wind variability or Fynbos vegetation expansions. Other Fynbos indicators did not display such trend (Fig. 4), suggesting that Restionaceae variability between 100 and 24 ka were more likely the result of enhanced variability of southeast trade winds. Restionaceae pollen percentage data from a record 2° North of our marine site also showed comparable increases in the amplitude of millennial-scale changes (Shi et al., 2001). Grain-size wind strength tracers from the Walvis Ridge displayed enhanced millennial-scale variability, although only after ca. 80 ka (Stuut et al., 2002). An analysis of BUS dynamics over the past 190 ka found increased millennial-scale variability of wind strength after ca. 100 ka and the windiest conditions in this zone during MIS 4 and 3 (Stuut et al., 2002). Such millennial-scale atmospheric reorganisations are recorded in the pollen-based DCA analysis as rapid biome shifts in southwestern Africa.

5 Conclusions

Terrestrial and marine markers from the marine core MD96-2098 documented expansions of the Nama-Karoo and fine-leaved savanna during MIS 5e, 5c and 5a warm

362

substages. Northwestern expansions of the Nama-Karoo and Fn-LSav are potentially linked to the reduction of BUS and a local increase in humidity in the desert area, while aridification increased at a regional scale. Towards the east, Nama-Karoo and Fn-LSav expansions probably resulted from increased subtropical high pressure, a northward shift of the ITCZ, and reduced austral-summer precipitation. Nama-Karoo and Fn-LSav expansions to the southern boundary are possibly associated with southern displacement of the westerlies and the subtropical front, decreasing austral-winter precipitation.

During glacial isotopic stages MIS 6, 4 and 3, Fynbos biome expansions are probably linked to the increased influence of the southern westerlies and austral-winter precipitation in southwestern Africa. Our pollen record also suggested that warm-cold or cold-warm transitions between isotopic stages and substages were punctuated by short increases in humidity. Increased variability of vegetation changes at millennial timescales ca. 100 ka was also documented and could be associated with previously-identified enhanced variability of the southeastern trade winds.

Interglacial-glacial southern Africa biome dynamics were linked to atmospheric and oceanic dynamics resulting from changes in global ice volume and precession at orbital timescales. Atmospheric configurations with westerly winds shifted southwards relative to today have been suggested for other interglacials (Peeters et al., 2004) and are projected for the end of 21st-century under current global warming (Beal et al., 2011). This is likely to reduce austral-winter precipitation over southern Africa and favour expansions of the Nama-Karoo at the expense of the winter-rain fed Fynbos and Succulent-Karoo biomes. However, taking the current orbital configuration alone, the Nama-Karoo and Fn-LSav in southern Africa might naturally remain relatively reduced for several millennial ahead.

**The Supplement related to this article is available online at
doi:10.5194/cpd-11-345-2015-supplement.**

363

Acknowledgements. We are grateful to L. Scott for giving us access to the pollen reference collection at the University of the Free State, Bloemfontein, South Africa. We also thank K. Gajewski and the African pollen database for complementary surface data. We acknowledge the Artemis program for support for radiocarbon dates at the Laboratoire de Mesure du Carbone 14. We thank Murielle Georget and Marie H el ene Castera for sample preparation and pollen extraction, Linda Rossignol for foraminifera preparation for ¹⁴C dating, Ludovic Devaux for help with the surface-sample dataset, and Will Banks for English proof reading. The marine core was retrieved during NAUSICAA oceanographic cruise (IMAGES II). This work was funded by the European Research Council Grant TRACSYMBOLS no. 249587 <http://tracsymbols.eu/>.

References

- Archibald, S., Scholes, R. J., Roy, D. P., Roberts, G., and Boschetti, L.: Southern African fire regimes as revealed by remote sensing, *Int. J. Wildland Fire*, 19, 861–878, doi:10.1071/WF10008, 2010.
- Beal, L. M. and Bryden, H. L.: The velocity and vorticity structure of the Agulhas Current at 32° S, *J. Geophys. Res.-Oceans*, 104, 5151–5176, doi:10.1029/1998jc900056, 1999.
- Beal, L. M., De Ruijter, W. P. M., Biastoch, A., and Zahn, R.: On the role of the Agulhas system in ocean circulation and climate, *Nature*, 472, 429–436, doi:10.1038/nature09983, 2011.
- Bereiter, B., L uthi, D., Siegrist, M., Sch ubach, S., Stocker, T. F., and Fischer, H.: Mode change of millennial CO₂ variability during the last glacial cycle associated with a bipolar marine carbon seesaw, *P. Natl. Acad. Sci. USA*, 109, 9755–9760, doi:10.1073/pnas.1204069109, 2012.
- Bertrand, P., Balut, Y., Schneider, R., Chen, M. T., Rogers, J., and Shipboard Scientific Party: Scientific Report of the NAUSICAA-IMAGES II Coring Cruise, Les rapports de campagne   la mer   bord du Marion-Dufresne, URA CNRS 197, Universit  Bordeaux 1, D partement de Geologie et Oceanographie, Talence, France, 382 pp., 1996.
- Bertrand, P., Giraudeau, J., Malaize, B., Martinez, P., Gallinari, M., Pedersen, T. F., Pierre, C., and V nec-Peyr , M. T.: Occurrence of an exceptional carbonate dissolution episode during early glacial isotope stage 6 in the Southeastern Atlantic, *Mar. Geol.*, 180, 235–248, doi:10.1016/s0025-3227(01)00216-x, 2002.

364

- Bertrand, P., Pedersen, T. F., Schneider, R., Shimmield, G., Lallier-Verges, E., Disnar, J. R., Massias, D., Villanueva, J., Tribovillard, N., Huc, A. Y., Giraud, X., Pierre, C., and Vénec-Peyre, M.-T.: Organic-rich sediments in ventilated deep-sea environments: relationship to climate, sea level, and trophic changes, *J. Geophys. Res.*, 108, 3045, doi:10.1029/2000JC000327, 2003.
- 5 Biastoch, A., Böning, C. W., and Lutjeharms, J. R. E.: Agulhas leakage dynamics affects decadal variability in Atlantic overturning circulation, *Nature*, 456, 489–492, 2008.
- Chase, B. M. and Meadows, M. E.: Late Quaternary dynamics of southern Africa's winter rainfall zone, *Earth-Sci. Rev.*, 84, 103–138, doi:10.1016/j.earscirev.2007.06.002, 2007.
- 10 Chen, M.-T., Chang, Y.-P., Chang, C.-C., Wang, L.-W., Wang, C.-H., and Yu, E.-F.: Late Quaternary sea-surface temperature variations in the southeast Atlantic: a planktic foraminifer faunal record of the past 600 000 yr (IMAGES II MD962085), *Mar. Geol.*, 180, 163–181, doi:10.1016/s0025-3227(01)00212-2, 2002.
- Collins, J. A., Schefuß, E., Govin, A., Mulitza, S., and Tiedemann, R.: Insolation and glacial–interglacial control on southwestern African hydroclimate over the past 140 000 years, *Earth Planet. Sc. Lett.*, 398, 1–10, doi:10.1016/j.epsl.2014.04.034, 2014.
- 15 Cowling, R. M. and Hilton-Taylor, C.: Phytogeography, flora and endemism, in: *The Karoo. Ecological Patterns and Processes*, edited by: Dean, W. R. J. and Milton, S., Cambridge University Press, Cambridge, UK, 42–56, 2009.
- 20 Cowling, R. M., Esler, K. J., Midgley, G. F., and Honig, M. A.: Plant functional diversity, species diversity and climate in arid and semi-arid southern Africa, *J. Arid Environ.*, 27, 141–158, 1994.
- Cowling, R. M., Richardson, D. M., and Mustart, P. J.: Fynbos, in: *Vegetation of Southern Africa*, edited by: Cowling, R. M., Richardson, D. M., and Pierce, S. M., Cambridge University Press, Cambridge, UK, 99–130, 1997a.
- 25 Cowling, R. M., Richardson, D. M., and Pierce, S. M.: *Vegetation of Southern Africa*, Cambridge University Press, Cambridge, UK, 615 pp., 1997b.
- Daniau, A.-L., Sánchez Goñi, M. F., Martinez, P., Urrego, D. H., Bout-Roumazielles, V., Desprat, S., and Marlon, J. R.: Orbital-scale climate forcing of grassland burning in southern Africa, *P. Natl. Acad. Sci. USA*, 110, 5069–5073, doi:10.1073/pnas.1214292110, 2013.
- 30 Dewar, G., Reimer, P. J., Sealy, J., and Woodborne, S.: Late-Holocene marine radiocarbon reservoir correction (ΔR) for the west coast of South Africa, *Holocene*, 22, 1481–1489, doi:10.1177/0959683612449755, 2012.

- Drysdale, R. N., Zanchetta, G., Hellstrom, J. C., Fallick, A. E., McDonald, J., and Cartwright, I.: Stalagmite evidence for the precise timing of North Atlantic cold events during the early last glacial, *Geology*, 35, 77–80, 2007.
- 5 Dupont, L. M.: Orbital scale vegetation change in Africa, *Quaternary Sci. Rev.*, 30, 3589–3602, doi:10.1016/j.quascirev.2011.09.019, 2011.
- Dupont, L. M. and Behling, H.: Land–sea linkages during deglaciation: high-resolution records from the eastern Atlantic off the coast of Namibia and Angola (ODP site 1078), *Quatern. Int.*, 148, 19–28, doi:10.1016/j.quaint.2005.11.004, 2006.
- 10 Dupont, L. M. and Wyputta, U.: Reconstructing pathways of aeolian pollen transport to the marine sediments along the coastline of SW Africa, *Quaternary Sci. Rev.*, 22, 157–174, 2003.
- Dupont, L. M., Behling, H., Jahns, S., Marret, F., and Kim, J.-H.: Variability in glacial and Holocene marine pollen records offshore from west southern Africa, *Veg. Hist. Archaeobot.*, 16, 87–100, doi:10.1007/s00334-006-0080-8, 2007.
- 15 Dupont, L. M., Caley, T., Kim, J.-H., Castañeda, I., Malaizé, B., and Giraudeau, J.: Glacial–interglacial vegetation dynamics in South Eastern Africa coupled to sea surface temperature variations in the Western Indian Ocean, *Clim. Past*, 7, 1209–1224, doi:10.5194/cp-7-1209-2011, 2011.
- EPICA: One-to-one coupling of glacial climate variability in Greenland and Antarctica, *Nature*, 444, 195–198, doi:10.1038/nature05301, 2006.
- 20 Faegri, K. and Iversen, J.: *Textbook of Pollen Analysis*, 4th edn., Wiley, Chichester, 328 pp., 1989.
- González, C. and Dupont, L. M.: Tropical salt marsh succession as sea-level indicator during Heinrich events, *Quaternary Sci. Rev.*, 28, 939–946, doi:10.1016/j.quascirev.2008.12.023, 2009.
- 25 Govin, A., Holzwarth, U., Heslop, D., Ford Keeling, L., Zabel, M., Mulitza, S., Collins, J. A., and Chiessi, C. M.: Distribution of major elements in Atlantic surface sediments (36° N–49° S): imprint of terrigenous input and continental weathering, *Geochem. Geophys. Geosy.*, 13, Q01013, 2012.
- 30 Henderson, G. M. and Slowey, N. C.: Evidence from U-Th dating against Northern Hemisphere forcing of the penultimate deglaciation, *Nature*, 404, 61–66, doi:10.1038/35003541, 2000.
- Heusser, L. and Balsam, W. L.: Pollen distribution in the northeast Pacific Ocean, *Quaternary Res.*, 7, 45–62, doi:10.1016/0033-5894(77)90013-8, 1977.

- Hooghiemstra, H., Agwu, C. O. C., and Beug, H.-J.: Pollen and spore distribution in recent marine sediments: a record of NW-African seasonal wind patterns and vegetation belts, *Meteor Forschungs-Ergebnisse C*, 40, 87–135, 1986.
- Hooghiemstra, H., Stalling, H., Agwu, C. O. C., and Dupont, L. M.: Vegetational and climatic changes at the northern fringe of the Sahara 250 000–5000 years BP: evidence from 4 marine pollen records located between Portugal and the Canary Islands, *Rev. Palaeobot. Palyno.*, 74, 1–53, doi:10.1016/0034-6667(92)90137-6, 1992.
- Hughen, K., Baillie, M., Bard, E., Bayliss, A., Beck, J., Bertrand, C., Blackwell, P., Buck, C., Burr, G., Cutler, K., Damon, P., Edwards, R., Fairbanks, R., Friedrich, M., Guilderson, T., Kromer, B., McCormac, F., Manning, S., Ramsey, C. B., Reimer, P., Reimer, R., Remmele, S., Southon, J., Stuiver, M., Talamo, S., Taylor, F., van der Plicht, J., and Weyhenmeyer, C.: Marine04 Marine radiocarbon age calibration, 26–0 ka BP, *Radiocarbon*, 46, 1059–1086, 2004.
- Huntley, B., Midgley, G. F., Barnard, P., and Valdes, P. J.: Suborbital climatic variability and centres of biological diversity in the Cape region of southern Africa, *J. Biogeogr.*, 41, 1338–1351, 2014.
- Imhoff, M. L., Bounoua, L., Ricketts, T., Loucks, C., Harriss, R., and Lawrence, W. T.: Global patterns in human consumption of net primary production, *Nature*, 429, 870–873, 2004.
- Jurgens, N., Burke, A., Seely, M. K., and Jacobson, K. M.: Desert, in: *Vegetation of Southern Africa*, edited by: Cowling, R. M., Richardson, D. M., and Pierce, S. M., Cambridge University Press, Cambridge, 189–214, 1997.
- Kirst, G. J., Schneider, R. R., Müller, P. J., von Storch, I., and Wefer, G.: Late Quaternary temperature variability in the Benguela current system derived from alkenones, *Quaternary Res.*, 52, 92–103, doi:10.1006/qres.1999.2040, 1999.
- Laskar, J.: The chaotic motion of the solar system: a numerical estimate of the chaotic zones, *Icarus*, 88, 266–291, 1990.
- Leroy, S. and Dupont, L.: Development of vegetation and continental aridity in northwestern Africa during the Late Pliocene: the pollen record of ODP site 658, *Palaeogeogr. Palaeoclimatol.*, 109, 295–316, doi:10.1016/0031-0182(94)90181-3, 1994.
- Lisiecki, L. E. and Raymo, M. E.: A Pliocene–Pleistocene stack of 57 globally distributed benthic $\delta^{18}\text{O}$ records, *Paleoceanography*, 20, PA1003, doi:10.1029/2004pa001071, 2005.
- Lutjeharms, J. R. E. and Meeuwis, J. M.: The extent and variability of South-East Atlantic upwelling, *S. Afr. J. Marine Sci.*, 5, 51–62, doi:10.2989/025776187784522621, 1987.

- Lyle, M., Heusser, L., Ravelo, C., Yamamoto, M., Barron, J., Diffenbaugh, N. S., Herbert, T., and Andreasen, D.: Out of the tropics: the Pacific, Great Basin Lakes, and Late Pleistocene water cycle in the western United States, *Science*, 337, 1629–1633, 2012.
- Masson-Delmotte, V., Stenni, B., Pol, K., Braconnot, P., Cattani, O., Falourd, S., Kageyama, M., Jouzel, J., Landais, A., Minster, B., Barnola, J. M., Chappellaz, J., Krinner, G., Johnsen, S., Röthlisberger, R., Hansen, J., Mikolajewicz, U., and Otto-Bliesner, B.: EPICA Dome C record of glacial and interglacial intensities, *Quaternary Sci. Rev.*, 29, 113–128, 2010.
- McCune, B. and Grace, J. B.: *Analysis of Ecological Communities*, MjM, Glenden Beach, OR, 300 pp., 2002.
- Meadows, M. E., Chase, B. M., and Seliane, M.: Holocene palaeoenvironments of the Cederberg and Swartruggens mountains, Western Cape, South Africa: pollen and stable isotope evidence from hyrax dung middens, *J. Arid Environ.*, 74, 786–793, doi:10.1016/j.jaridenv.2009.04.020, 2010.
- Mills, S. C., Grab, S. W., Rea, B. R., Carr, S. J., and Farrow, A.: Shifting westerlies and precipitation patterns during the Late Pleistocene in southern Africa determined using glacier reconstruction and mass balance modelling, *Quaternary Sci. Rev.*, 55, 145–159, doi:10.1016/j.quascirev.2012.08.012, 2012.
- Milton, S. J., Yeaton, R. I., Dean, W. R. J., and Vlok, J. H. J.: Succulent karoo, in: *Vegetation of Southern Africa*, edited by: Cowling, R. M., Richardson, D. M., and Pierce, S. M., Cambridge University Press, Cambridge, 131–166, 1997.
- O'Connor, T. G. and Breckenkamp, G. J.: Grassland, in: *Vegetation of Southern Africa*, edited by: Cowling, R. M., Richardson, D. M., and Pierce, S. M., Cambridge University Press, Cambridge, UK, 215–257, 1997.
- Palmer, A. R. and Hoffman, M. T.: Nama-Karoo, in: *Vegetation of Southern Africa*, edited by: Cowling, R. M., Richardson, D. M., and Pierce, S. M., Cambridge University Press, Cambridge, 167–188, 1997.
- Partridge, T. C., Demenocal, P. B., Lorentz, S. A., Paiker, M. J., and Vogel, J. C.: Orbital forcing of climate over South Africa: a 200 000 year rainfall record from the pretoria saltpan, *Quaternary Sci. Rev.*, 16, 1125–1133, doi:10.1016/S0277-3791(97)00005-X, 1997.
- Peeters, F. J. C., Acheson, R., Brummer, G.-J. A., de Ruijter, W. P. M., Schneider, R. R., Ganssen, G. M., Ufkes, E., and Kroon, D.: Vigorous exchange between the Indian and Atlantic oceans at the end of the past five glacial periods, *Nature*, 430, 661–665, doi:10.1038/nature02785, 2004.

- Petit, J. R., Jouzel, J., Raynaud, D., Barkov, N. I., Barnola, J.-M., Basile, I., Bender, M., and Chappellaz, J.: Climate and atmospheric history of the past 420 000 years from the Vostok ice core, Antarctica, *Nature*, 399, 429–436, 1999.
- Pichevin, L., Martinez, P., Bertrand, P., Schneider, R., Giraudeau, J., and Emeis, K.: Nitrogen cycling on the Namibian shelf and slope over the last two climatic cycles: local and global forcings, *Paleoceanography*, 20, PA2006, doi:10.1029/2004pa001001, 2005.
- Reimer, P. J., Bard, E., Bayliss, A., Beck, J. W., Blackwell, P. G., Bronk Ramsey, C., Buck, C. E., Cheng, H., Edwards, R. L., Friedrich, M., Grootes, P. M., Guilderson, T. P., Haflidason, H., Hajdas, I., Hatté, C., Heaton, T. J., Hoffmann, D. L., Hogg, A. G., Hughen, K. A., Kaiser, K. F., Kromer, B., Manning, S. W., Niu, M., Reimer, R. W., Richards, D. A., Scott, E. M., Southon, J. R., Staff, R. A., Turney, C. S. M., and Plicht, J. v. d.: IntCal13 and Marine13 radiocarbon age calibration curves 0–50000 years cal BP, *Radiocarbon*, 55, 1869–1887, 2013.
- Rogers, J. and Rau, A. J.: Surficial sediments of the wave-dominated Orange River Delta and the adjacent continental margin off south-western Africa, *S. Afr. J. Marine Sci.*, 28, 511–524, doi:10.2989/18142320609504202, 2006.
- Röthlisberger, R., Mudelsee, M., Bigler, M., de Angelis, M., Fischer, H., Hansson, M., Lambert, F., Masson-Delmotte, V., Sime, L., Udisti, R., and Wolff, E. W.: The Southern Hemisphere at glacial terminations: insights from the Dome C ice core, *Clim. Past*, 4, 345–356, doi:10.5194/cp-4-345-2008, 2008.
- Ruddiman, W. F.: Orbital changes and climate, *Quaternary Sci. Rev.*, 25, 3092–3112, 2006.
- Rutherford, M. C.: Categorization of biomes, in: *Vegetation of Southern Africa*, edited by: Cowling, R. M., Richardson, D. M., and Pierce, S. M., Cambridge University Press, Cambridge, UK, 91–98, 1997.
- Sanchez Goñi, M. F. and Harrison, S. P.: Millennial-scale climate variability and vegetation changes during the Last Glacial: concepts and terminology, *Quaternary Sci. Rev.*, 29, 2823–2827, 2010.
- Sánchez Goñi, M. A. F., Turon, J.-L., Eynaud, F., and Gendreau, S.: European climatic response to millennial-scale changes in the atmosphere–ocean system during the Last Glacial Period, *Quaternary Res.*, 54, 394–403, doi:10.1006/qres.2000.2176, 2000.
- Sánchez Goñi, M. F., Eynaud, F., Turon, J. L., and Shackleton, N. J.: High resolution palynological record off the Iberian margin: direct land–sea correlation for the last interglacial complex, *Earth Planet. Sc. Lett.*, 171, 123–137, doi:10.1016/s0012-821x(99)00141-7, 1999.

- Scholes, R. J.: Savanna, in: *Vegetation of Southern Africa*, edited by: Cowling, R. M., Richardson, D. M., and Pierce, S. M., Cambridge University Press, Cambridge, UK, 258–277, 1997.
- Scott, L.: Late Quaternary fossil pollen grains from the Transvaal, South Africa, *Rev. Palaeobot. Palyno.*, 36, 241–268, 1982.
- Scott, L., Marais, E., and Brook, G. A.: Fossil hyrax dung and evidence of Late Pleistocene and Holocene vegetation types in the Namib Desert, *J. Quaternary Sci.*, 19, 829–832, doi:10.1002/jqs.870, 2004.
- Scott, L., Neumann, F. H., Brook, G. A., Bousman, C. B., Norström, E., and Metwally, A. A.: Terrestrial fossil-pollen evidence of climate change during the last 26 thousand years in Southern Africa, *Quaternary Sci. Rev.*, 32, 100–118, doi:10.1016/j.quascirev.2011.11.010, 2012.
- Shi, N., Dupont, L. M., Beug, H.-J., and Schneider, R.: Correlation between vegetation in south-western Africa and oceanic upwelling in the past 21 000 years, *Quaternary Res.*, 54, 72–80, doi:10.1006/qres.2000.2145, 2000.
- Shi, N., Schneider, R., Beug, H.-J., and Dupont, L. M.: Southeast trade wind variations during the last 135 kyr: evidence from pollen spectra in eastern South Atlantic sediments, *Earth Planet. Sc. Lett.*, 187, 311–321, doi:10.1016/s0012-821x(01)00267-9, 2001.
- Southon, J., Kashgarian, M., Fontugne, M., Metivier, B., and Yim, W. W.-S.: Marine reservoir corrections for the Indian Ocean and Southeast Asia, *Radiocarbon*, 44, 167–180, 2002.
- Stuut, J.-B. W. and Lamy, F.: Climate variability at the southern boundaries of the Namib (south-western Africa) and Atacama (northern Chile) coastal deserts during the last 120 000 yr, *Quaternary Res.*, 62, 301–309, doi:10.1016/j.yqres.2004.08.001, 2004.
- Stuut, J.-B. W., Prins, M. A., Schneider, R. R., Weltje, G. J., Jansen, J. H. F., and Postma, G.: A 300 kyr record of aridity and wind strength in southwestern Africa: inferences from grain-size distributions of sediments on Walvis Ridge, SE Atlantic, *Mar. Geol.*, 180, 221–233, doi:10.1016/s0025-3227(01)00215-8, 2002.
- Toggweiler, J. R. and Russell, J.: Ocean circulation in a warming climate, *Nature*, 451, 286–288, 2008.
- Tyson, P. D.: Atmospheric circulation changes and palaeoclimates of southern Africa, *S. Afr. J. Sci.*, 95, 194–201, 1999.
- Tyson, P. D. and Preston-Whyte, R. A.: *The Weather and Climate of Southern Africa*, Oxford University Press Southern Africa, Cape Town, 396 pp., 2000.

- Waelbroeck, C., Frank, N., Jouzel, J., Parrenin, F., Masson-Delmotte, V., and Genty, D.: Transferring radiometric dating of the last interglacial sea level high stand to marine and ice core records, *Earth Planet. Sc. Lett.*, 265, 183–194, 2008.
- Wang, X., Auler, A. S., Edwards, R. L., Cheng, H., Cristalli, P. S., Smart, P. L., Richards, D. A., and Shen, C.-C.: Wet periods in northeastern Brazil over the past 210 kyr linked to distant climate anomalies, *Nature*, 432, 740–743, 2004.
- Weldeab, S., Stuut, J.-B. W., Schneider, R. R., and Siebel, W.: Holocene climate variability in the winter rainfall zone of South Africa, *Clim. Past*, 9, 2347–2364, doi:10.5194/cp-9-2347-2013, 2013.
- White, F.: The vegetation of Africa: a descriptive memoir to accompany the Unesco/AETFAT/UNSO vegetation map of Africa, Paris, 356, 356 pp., 1983.
- Wuillez, M.-N., Levavasseur, G., Daniau, A.-L., Kageyama, M., Urrego, D. H., Sánchez-Gofñi, M.-F., and Hanquiez, V.: Impact of precession on the climate, vegetation and fire activity in southern Africa during MIS4, *Clim. Past*, 10, 1165–1182, doi:10.5194/cp-10-1165-2014, 2014.

371

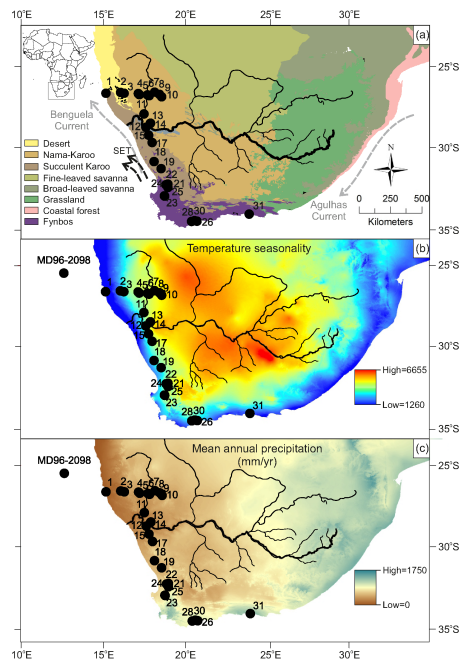


Figure 1. (a) Map of biomes of southern Africa based on Mucina et al. (2007) and modified using the savanna classification by Scholes (1997), location of the Orange River and major tributaries, oceanic currents (grey arrows) and southeastern trade winds (black arrows). Temperature seasonality (b) and annual precipitation in mm yr^{-1} (c) extracted from the WorldClim dataset (Hijmans et al., 2005). Black dots indicate location of marine core MD96-2098 and numbers indicate the location of surface sample collection points described in Table S1.

372

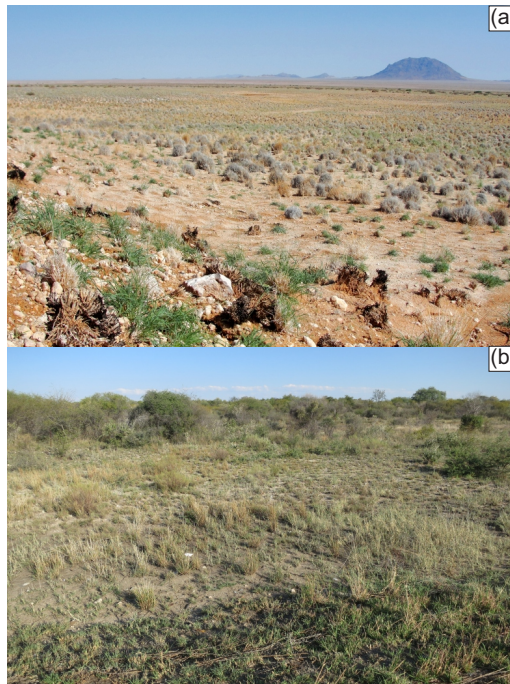


Figure 2. (a) Grass-dominated Nama-Karoo vegetation near Grunau, Namibia. Photo: D.H. Urrego. (b) Grass-dominated fine-leaved savanna vegetation in the Kalahari region of Namibia. Photo: F. D'Errico.

373

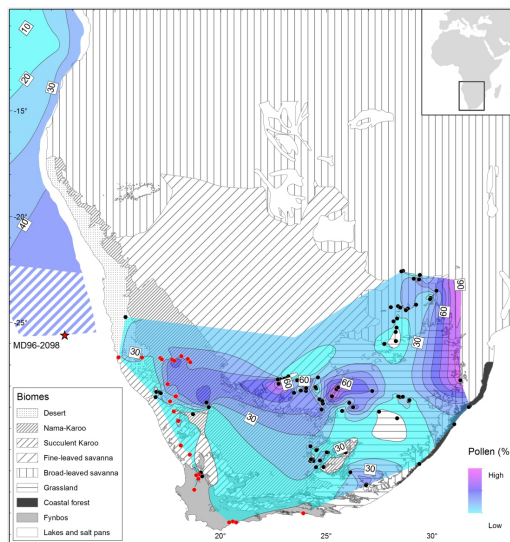


Figure 3. Poaceae pollen percentage iso-lines drawn over biome units of southern Africa (modified from Scholes, 1997; Mucina et al., 2007). The broad-leaved savanna distribution includes the Mopane and mixed savannas described by Scholes (1997). Iso-lines are plotted based on pollen percentage data from surface samples analysed in this study (red dots) and pollen spectra from other samples previously published and extracted from the African Pollen Database (black dots) (Gajewski et al., 2002). Poaceae pollen percentage in the marine domain are redrawn from Dupont and Wyputta (2003) and extended to latitude 25° S using two MD96-2098 core-top samples (hatched).

374

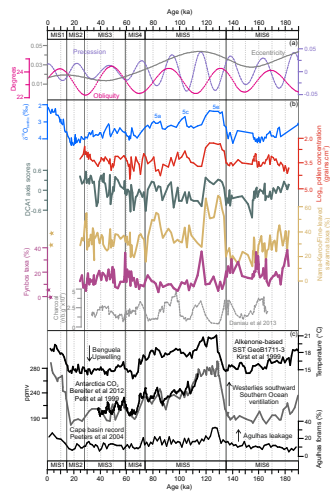


Figure 4. Comparison of terrestrial, atmospheric and oceanic markers for southern Africa between 190 and 24 ka. **(a)** Orbital parameters plotted for latitude 25°36' S using La2004 (Laskar et al., 2004). **(b)** Stable oxygen profile of benthic foraminifera *Cibicidoides wuellerstorfi* (Bertrand et al., 2002), log-transformed total pollen concentration, detrended correspondence analysis Axis1 scores, pollen percentages of indicator taxa for Nama-Karoo and fine-leaved savanna (Acanthaceae, Aizoaceae, Crassulaceae, Euphorbia, Poaceae, and *Tribulus*,) and Fynbos (*Artemisia*-type, Ericaceae, Passerina, *Protea*, and *Stoebe*-type), charcoal concentrations in number of particles per gram (nb g^{-1}) from marine core MD96-2098 plotted against age in ka (thousands of calibrated/calendar years before present). Stars on the left correspond to percentage of pollen taxa in two top-core samples dating 530 and 1060 calibrated years before present. **(c)** Independent climatic records discussed in the text. Gray curve: low-resolution CO_2 record from Vostok (Petit et al., 1999); black curve: high-resolution CO_2 record from Bereiter et al. (2012). Stage boundary ages for 3/2, 4/3, and 5/4 from (Sanchez Goñi and Harrison, 2010) and 6/5 from (Henderson and Slowey, 2000).

375

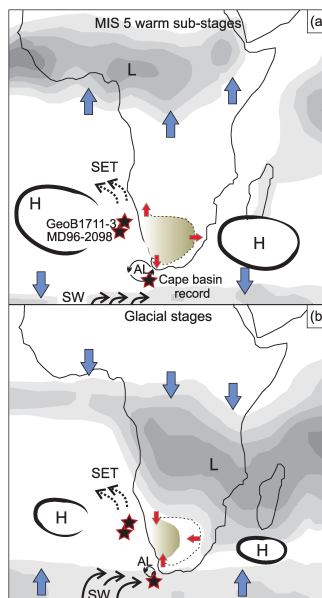


Figure 5. Schematic and simplified configuration of vegetation, atmospheric, and oceanic systems over southern Africa during **(a)** the MIS 5 warm sub-stages, and **(b)** glacial isotopic stages. Rainfall is illustrated as grey areas showing the current configuration of tropical and subtropical convection systems using average austral-winter **(a)** and austral-summer **(b)** precipitation data between 1979 and 1995 from the International Research Institute for Climate Prediction (<http://iri.ldeo.columbia.edu>). L: tropical low-pressure systems, H: subtropical high-pressure systems, SET: southeast trade winds, SW: southern westerlies, AL: Agulhas leakage. Stars indicate the location of marine records discussed in the text and blue arrows indicate the direction of pressure system migration. Red arrows and brown shaded area indicate hypothesized expansion **(a)** or contraction of the Nama-Karoo and fine-leaved savanna **(b)**.

376